Development of a Targeted Inspection Plan for the Raccoon Mountain Pumped Storage Facility

Eric Scheibler, Senior Consulting Engineer[1], Bruno Fletcher, M.Sc., CFD Consulting Engineer[1], Tennessee Valley Authority[3]
[1]Quest Integrity Group, 1965 57th Court North Suite 100 Boulder, CO 80301
[3]Tennessee Valley Authority, 1101 Market Street LP 3P-C, Chattanooga, TN 37402

*Presented at the Hydrovision International Conference 2014, Nashville, Tennessee

Abstract

The Raccoon Mountain Pumped Storage Facility (RPS) in Chattanooga, TN is among the world's largest pumped storage hydroelectric power stations. Tennessee Valley Authority (TVA) operates RPS with four 415 MW reversible Francis units providing 1600 MW of generating capacity. TVA wanted to develop a long-term inspection program for critical equipment associated with the pressure boundaries along the waterway at RPS. The scope of this project encompassed components along the waterway beginning with the Penstock Tube Liner including the Spherical Ball Valve, Spiral Case, Wicket Gates, Headcover, Mechanical Shaft Seal, Wheel-pit piping, Draft Tube, and associated Manways. This paper covers the methodology that was used to develop inspection recommendations and intervals for RPS operating under power-generation mode. The project consisted of performing multiple types of analyses including: computational fluid dynamics (CFD), finite element analysis (FEA), and fitness-for-service assessments.

Laser scanning of one of the Francis units runner blade was performed to obtain the actual blade geometry as its span-wise profile, taper, and twist are not made available through traditional engineering drawings. A computer-aided design (CAD) model of the Francis unit was created using the laser scanned data and engineering drawings. The developed CAD model was used to create both CFD and FEA models for the Francis units.

A series of CFD models were developed to obtain steady state pressure distribution along multiple flow paths for a Francis unit. The pressures computed from CFD were

then prescribed as boundary conditions for the FEA models where stresses were calculated at various critical components within the unit. The stresses from the FEA analyses were extracted and used as primary stress inputs for critical crack size computations and fatigue life estimates for the fitness-for-service assessments. This approach was performed in accordance with *API 579-1/ASME FFS-1 Fitness-for-Service* guidelines and provided TVA with quantitative means to plan for regular inspections and end-of-life budgeting.

Introduction

The Raccoon Mountain Pumped Storage Facility (RPS) is situated on a site overlooking the Tennessee River in Chattanooga, Tennessee. RPS is Tennessee Valley Authority's (TVA) largest hydroelectric facility and has been service since 1978.

Figure 1: Aerial view of the Raccoon Mountain pumped storage reservoir [1]

RPS is a hydroelectric pump storage facility where water is pumped uphill to a manmade reservoir during the hours of low electricity demand, while water flows downhill when electricity is generated to meet the high demand. The RPS facility is operated by four 415 MW reversible Francis turbines with a rated head of 1,019 feet.

This project was conducted using a series of multidisciplinary engineering assessments that included computational fluid dynamics (CFD), finite element analysis (FEA), and fracture mechanics to accurately capture the physical response of the critical waterway

components and to evaluate the damage tolerance of these components to crack like flaws.

Laser scanning on one of the Francis unit's runner blade was performed to obtain accurate runner geometry. Three dimensional computer-aided design (CAD) models from the steel penstock liner to the draft tube were developed as starting point for both CFD and FEA models.

The pressures calculated from the CFD analyses were used to set the boundary conditions for various FEA models where stresses were calculated. The stresses from the FEA analyses were extracted and used as primary stress inputs for critical crack size computations and fatigue driven crack growth assessments. The results of these analyses were used to determine remaining life estimates of each component analyzed, providing TVA with quantitative means to plan for regular targeted inspections (locations and intervals) and component end-of-life budgeting.

Nearly twenty fluid and structural models were created to model critical pressure boundaries from the steel penstock liner to the draft tube. This paper focuses on the global and local CFD models developed to accurately determine waterway boundary pressures and as a specific example, the fitness-for-service evaluation of the concrete embedded spiral case.

Objectives

The main objective of this project was to provide TVA with a focused inspection plan based on quantitative evidence that is supported by a recognized engineering standard, for the critical pressure containing components along the waterway from the steel penstock liner through the draft tube.

Advantages of having a focused inspection plan are:

- Increase safety.
- Budgetary planning allowing for allocation of inspection resources.
- Decrease inspection costs while inspecting more components through targeted inspections. Traditional general inspection procedures are typically unable to cover the entire waterway components evaluated herein within a timely fashion and budget.
- Decrease the possibility of having costly unplanned shutdowns due to critical equipment failure.

Methodology

This project was conducted following the guidelines of the API 579-1/ASME FFS-1 Fitness-for-Service [2] standard. This standard was developed to provide assessments methodologies for a variety of damage mechanisms (e.g. corrosion, erosion, crack like flaws, etc.) found primarily in pressure containing equipment. Analyses conducted in accordance to this standard provide support for targeted inspection, maintenance and operational decisions to maintain long-term economic viability, and to ensure safety of plant personnel and the public while older critical equipment continues to operate

The following Sections describe the approach and methods used for evaluating the various waterway components in this project.

Site Visit

The project began with one of several site visits to the RPS facility. The initial visit consisted of discussions between Quest Integrity and TVA engineers regarding plant operation, historical precedence and present concerns. Approximately fifteen modes of operation and extreme events combined with fourteen critical waterway components created a combination of 210 possibilities to evaluate at RPS. Therefore, Quest Integrity and TVA engineers defined preliminary analyses that consisted of maximum steady state operation both in generation and pumping modes. These modes of operation were most documented and supported with historical testing data. This allowed for verification of the numerical models.

Additional site visits consisted of performing multiple walk-downs along the waterway, including the spiral case and draft tube sections of the Francis units. Photographs and measurements were taken to document the current conditions and any structural modifications. Engineering drawings and operational data were also collected during this phase of the project.

Laser scanning (Figure 2) and ultrasonic thickness measurements of one Francis unit's runner blade was conducted to obtain accurate runner geometry as the available engineering drawings did not include enough detail to recreate the geometry of the component.

Figure 2: Quest Integrity engineer conducting a 3D laser scan of the high pressure side of the runner blade.

An accurate representation of the runner was necessary since its profile and span-wise twist would have a significant effect on the predicted pressure distribution throughout the modeled waterway.

Geometry

A series of 3D geometry models of the critical waterway components were generated using SolidWorks [3] and Rhino [4] commercial CAD software. These models were developed using the information provided in the engineering drawings, as well as the laser scanned data that was gathered for the runner (Figure 3).

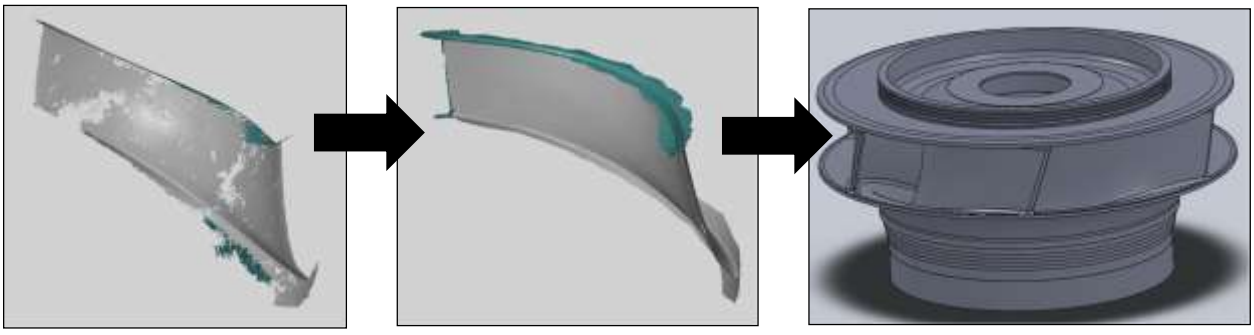

Figure 3: Using laser scan data and mechanical drawings, a 3D model of the runner was created.

The developed 3D geometry models included the steel penstock liner including the spherical ball valve, spiral case, stay vanes, wicket gates, headcover, mechanical shaft seal, wheel-pit piping, draft tube, and associated manways. Figure 4 shows one of the assembly CAD models that were developed for this project.

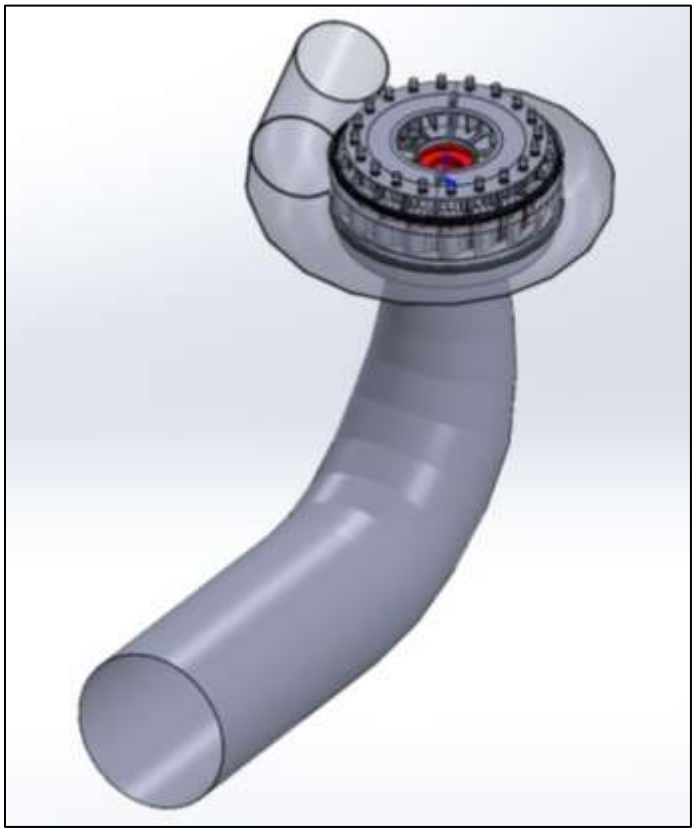

Figure 4: 3-D CAD assembly model for global CFD model

The 3D model geometry defined the surfaces for the various components to be subsequently analyzed by CFD to accurately calculate the pressure values along the pressure boundaries of the modeled waterway. The calculated pressure values would subsequently be mapped to the structural finite element models (FEM) for stress analysis.

Computational Fluid Dynamics (CFD) Modeling

Multiple steady-state CFD models were created to determine the pressure loads throughout the critical components of the unit. The predicted pressure loads were used to set the boundary conditions in the subsequent FEA modeling. The performed CFD modeling looked at the unit while operating under typical steady conditions for both the

power generation and pumping modes. The CFD analyses looked at the main flow path (i.e., the flow through spiral case, runner, and draft tube) as well as multiple secondary flow paths such as those encountered between runner and head cover, the runner and discharge ring, and associated manways. The modeling was conducted using inlet mass flow rates and outlet pressure values that were measured from operational field data.

The CFD modeling was conducted using Star-CCM+ [5], which is a validated commercial flow solver capable of modeling complex turbulent flows. The assumptions/physics included in the CFD modeling are as follows:

- Single phase fluid
- Steady state analysis
- Constant density water
- Gravitational effects
- k-ω SST turbulence model
- Rotation modeled as a moving reference frame.

Assumptions and simplifications were made in order to model the complex process of hydropower generation. Water was modeled as a single-phase liquid. This assumption is valid for all areas where the absolute pressure exceeds 0.26 psi at a water temperature of 60 degrees Fahrenheit [6] (i.e., valid for areas do not have cavitation).

The next assumption made was that of steady state flow. By performing a steady state analysis, the predicted pressure loading was averaged over time. This eliminated the cyclic loading effects of the flow, greatly reducing the computational time.

By assuming a constant density fluid, it is inherently implied that the fluid was modeled as being incompressible. This simplification significantly reduced the complexity of the system of equations being solved. Water is commonly accepted as an incompressible fluid.

Since nearly all flows of interest are highly turbulent in nature, the flow field cannot be solved without the use of a turbulence model. There are an abundance of turbulence models available, ranging in complexity. They are typically developed around a certain type of flow and correspondingly perform better for that particular flow. The *k-ω* SST model was chosen, as it is known to give good results for areas where the flow tends to separate from surfaces (as encountered in the rotating runner surfaces).

The moving reference frame method for modeling rotation uses principals of relative motion to keep the mesh stationary while numerically rotating the volume and shear effects of the walls contained in the region. This allows for the rotational effects (such as the Coriolis effect) to be modeled without incurring the computational cost of mesh motion.

The nature of the Francis unit geometry was conducive to developing two types of models. The first type were the global models, comprised of the main fluid flow path flowing from the spiral case through the stay vanes, wicket gates, runner, and draft tube. The global models were used to obtain the overall pressure distribution along the main flow path while operating under both power generation and pumping modes. These models neglected flow losses due to secondary flow paths. The overall geometry of the global models for the pumping and power generation modes were the same with the exception of the incidence angle setting for the wicket gates; the flow direction was also reversed depending if the unit was operating under power generation or pumping modes, as was the spin direction of the runner. An example of a global model used in this project is shown in Figure 5.

The models were verified using comparison to pressure measurements taken at various points along the waterway..

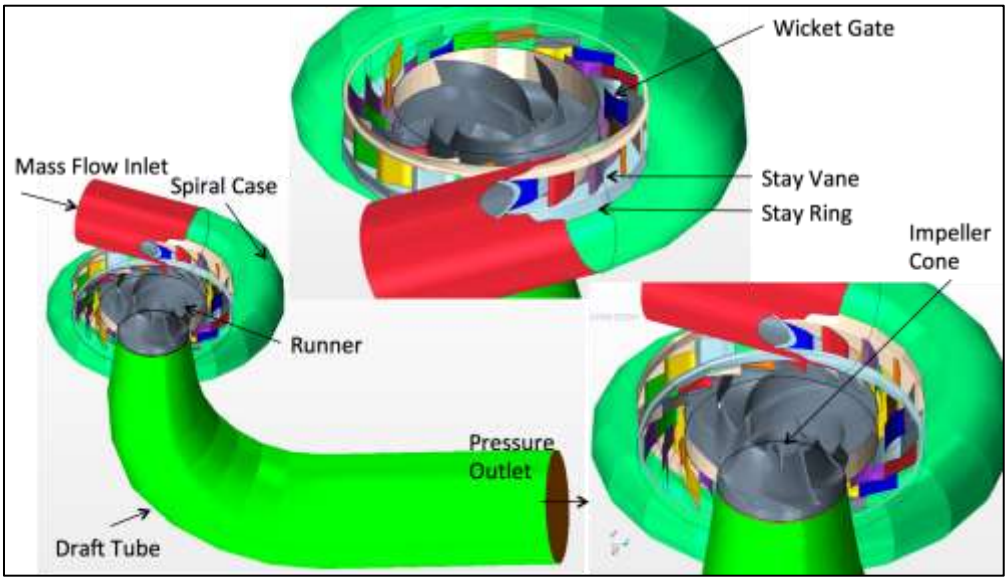

Figure 5: Global CFD model for power generation mode

The second type of CFD model were submodels used to obtain detailed flow solution along secondary flow paths, such as those encountered in between the head cover and

runner, as well as the flow within the cavities of the discharge ring assembly. The submodels used prescribed pressures and velocities at their inlets and outlets from the CFD solution of the global model. In order to map results from the global models to submodels it was imperative that these models shared the same coordinate system and adjacent computational domains. Figure 6 shows the submodel used to obtain detailed pressure distribution for the head cover and equalizer piping, as well its location in relationship to computation domain of the global model which prescribed its boundary conditions.

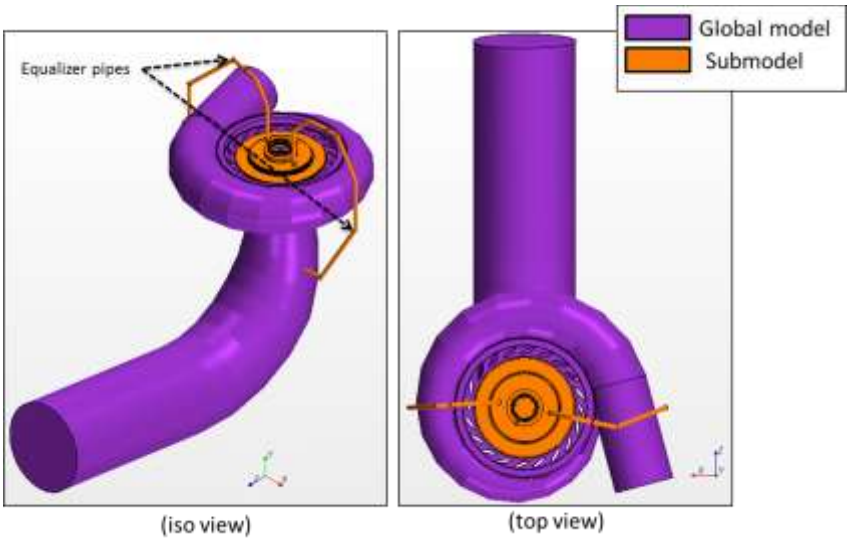

Figure 6: CFD submodel model to obtain head cover pressure

Stress Analysis

To accurately model the physical response of the pressure containing equipment along the waterway at RPS, finite element modeling was conducted using the Abaqus [7] FEA software. The structural models included the surrounding concrete where relevant. Table 1 provides a list of the waterway components modeled.

Table 1: Modeled waterway components.

Embedded	Non-Embedded
Steel penstock liner	Spherical ball valve
Spiral case	Spiral case manway
Stay rings	Headcover
Stay vanes	Mechanical shaft seal
Discharge ring	Equalizer piping
Draft tube	Wicket gates
	Bottom ring
	Draft tube manway

Examples of embedded and non-embedded finite element model are shown in Figure 7. The stress analyses considered the highest steady state condition for the generation (seventy percent gate opening) mode of operation. TVA and Quest Integrity engineers chose to pursue this approach for the following reasons:

- Achieve a more comprehensive understanding on how each modeled component individually responds when realistically modeled as a *system of components* subjected pressure loading calculated from fluid modeling.
- Structural evaluation of the critical waterway components subjected to peak steady state operation loads encountered during the majority of operational time to evaluate if the individual components response is elastic.
- The majority of historical data was recorded during these operation modes, which provide calibration and verification of numerical models.
- Provided preliminary basis to pursue other combinations of operational modes including transients.

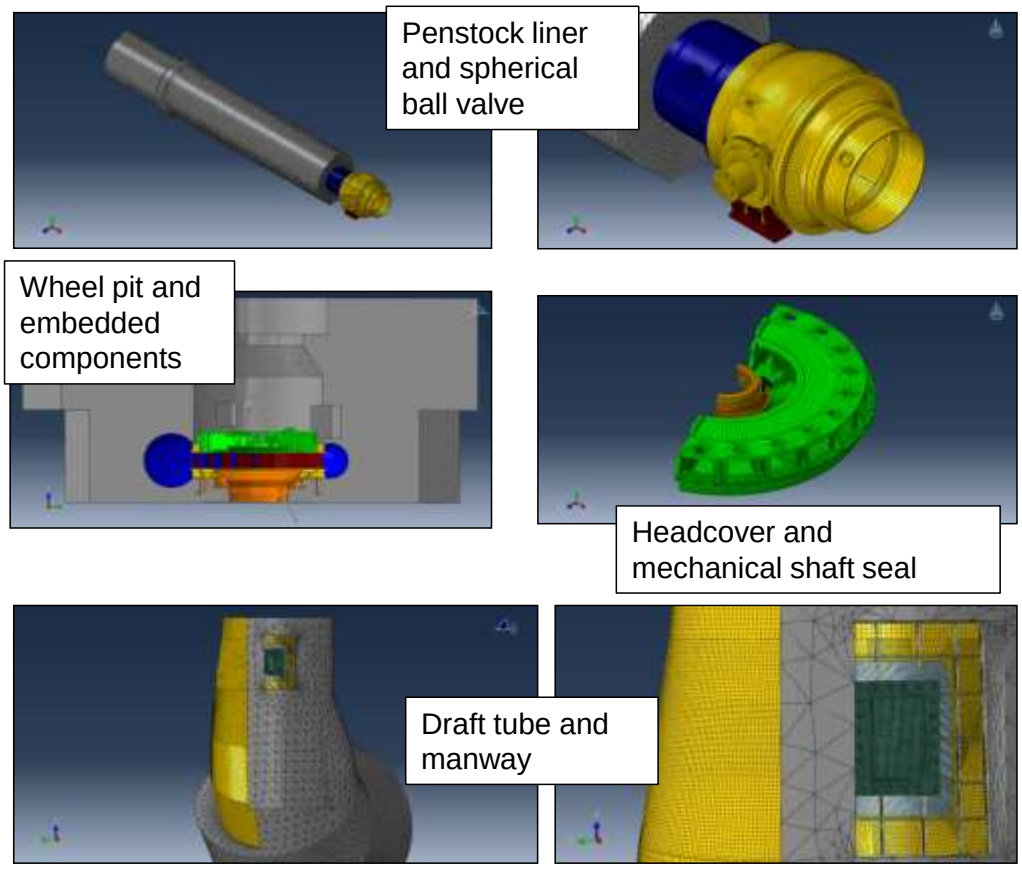

Figure 7: Example of finite element models for the RPS project.

Until additional transient analyses are conducted, stress results were scaled to peak measured pressure values associated with transient operation modes (e.g. pump start). This was to ensure that dynamic loading due to transients, for example pump start, were sufficiently accounted for, when evaluating the components in the subsequent fitness-for-service assessments.

Fitness-for-Service

A fitness-for-service (FFS) assessment is a multi-disciplinary approach to determine if a given structure is fit for continued service. The outcome of an FFS assessment is a decision to operate as is, repair, retire, and re-rate. The FFS approach also provides a quantitative means for determining and when and where to inspect.

Comprehensive guidelines for FFS assessments are contained in the API 579-1/ASME FFS-1 [2] (ASME FFS-1) standard, which is jointly published by the American Petroleum Institute (API) and the American Society for Mechanical Engineers (ASME).

This includes three levels of assessment for each damage mechanism outlined in the standard.

Level 1 is a simplified and conservative analysis that is used for initial screening purposes.

Level 2 is a basic engineering analysis that uses standard formulae to perform the FFS assessment. Typical Level 2 FFS calculations can be performed with a spreadsheet or custom software.

Level 3 is an advanced assessment that may include computational fluid dynamics and finite element simulation to obtain a detailed response of a structure, or a system of structures, comprised of complex geometries and subjected to complex applied loads. These analyses may involve two-dimensional (2D) or three-dimensional (3D) modeling to accurately determine the stresses in the damaged areas. These stresses can then be evaluated to determine suitability of the component for continued service.

A *Level 3* FFS *damage tolerance* approach was used to evaluate the critical waterway components from the steel penstock liner through the draft tube. The term damage tolerance typically refers to methodologies in which fracture mechanics analyses predict remaining life and quantify inspection intervals. This approach is usually applied to structures that are susceptible to time-dependent flaw growth (e.g. fatigue).

One of the first tasks of a damage tolerance analysis is the estimation of critical flaw sizes, which is described in the following section.

Crack Stability and Limiting Flaw Curves

The failure assessment diagram (FAD) method found in the ASME FFS-1 [2] standard describes the measure of acceptability of a component that contains a crack-like flaw. The FAD method considers both unstable (brittle) fracture and limit load (plastic overload). In a FFS of a crack-like flaw, the results from stress analyses, stress intensity factor and limit load solutions, material strength, and fracture toughness are combined to compute a non-dimensional toughness ratio, K_r, and load ratio, L_r. The computed K_r (vertical coordinate) and L_r (horizontal coordinate) point represents the crack-like flaw's acceptability. If the point falls on or below the FAD curve, the component is considered safe for continued operation. If the computed K_r and L_r point falls outside of the curve the component is considered unsafe for continued operation. An example of the FAD curve is shown in Figure 8. A point to the upper left of the FAD will fail by brittle fracture, while a point on the far right will fail by plastic collapse.

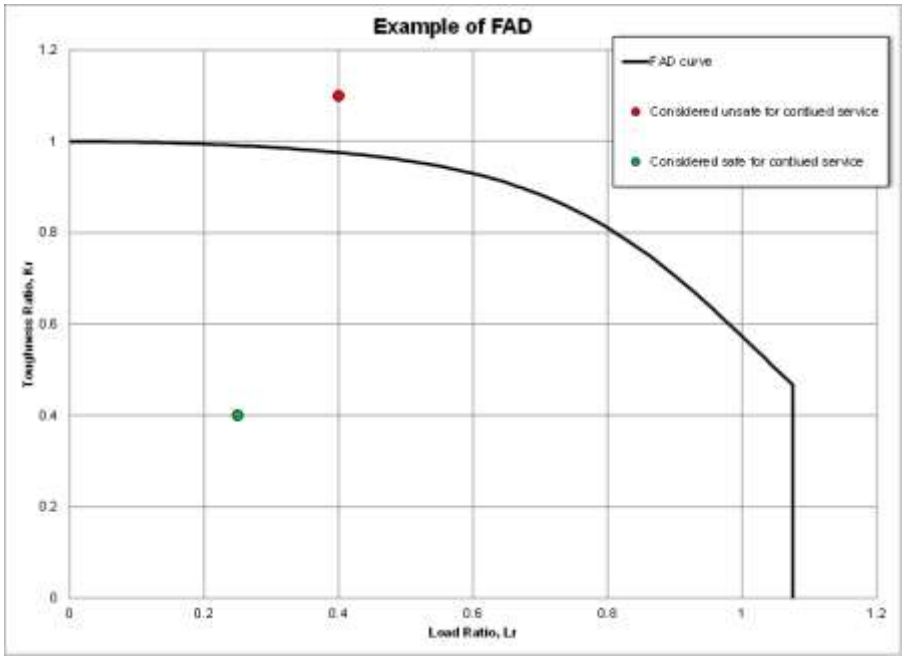

Figure 8: Example of FAD plot.

Alternatively, a technique exists for evaluating a component that has not been identified as having a crack-like flaw. This technique is based on the FAD method and evaluates a number of potential crack-like flaw depth-to-length aspect ratios. One way to represent this critical crack information is by plotting a limiting flaw curve (LFC) based on methods found in the ASME FFS-1 [2]. Combinations of flaw length and depth are determined which pose a risk for sudden failure due to brittle fracture or plastic collapse. Thus, these flaw dimensions represent points that fall exactly on the FAD. If the characteristic flaw dimensions (e.g. length, height) fall under the limiting flaw curve, then the flaw is considered acceptable. If the characteristic flaw dimensions fall outside the limiting flaw curve, then the flaw would be considered unacceptable. The limiting flaw curve provides a means to evaluate many combinations of potential flaw sizes. An example of the limiting flaw curve is shown in Figure 9.

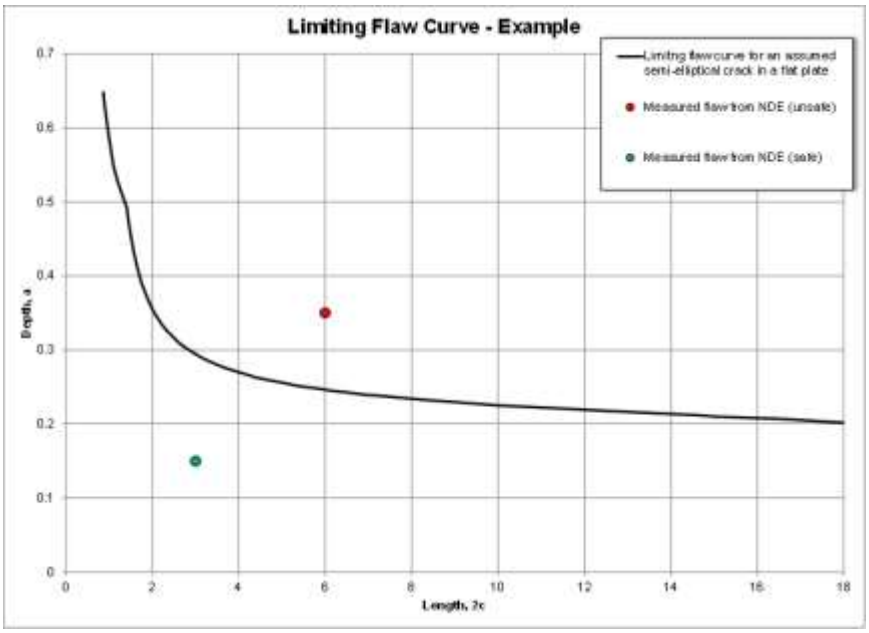

Figure 9: Example of limiting flaw curve plot.

Primary through thickness stress profiles from the FEA were scaled to account for affects due to transient loadings. This is an appropriately conservative approach that reduces the overall size of acceptable flaws (Figure 10).

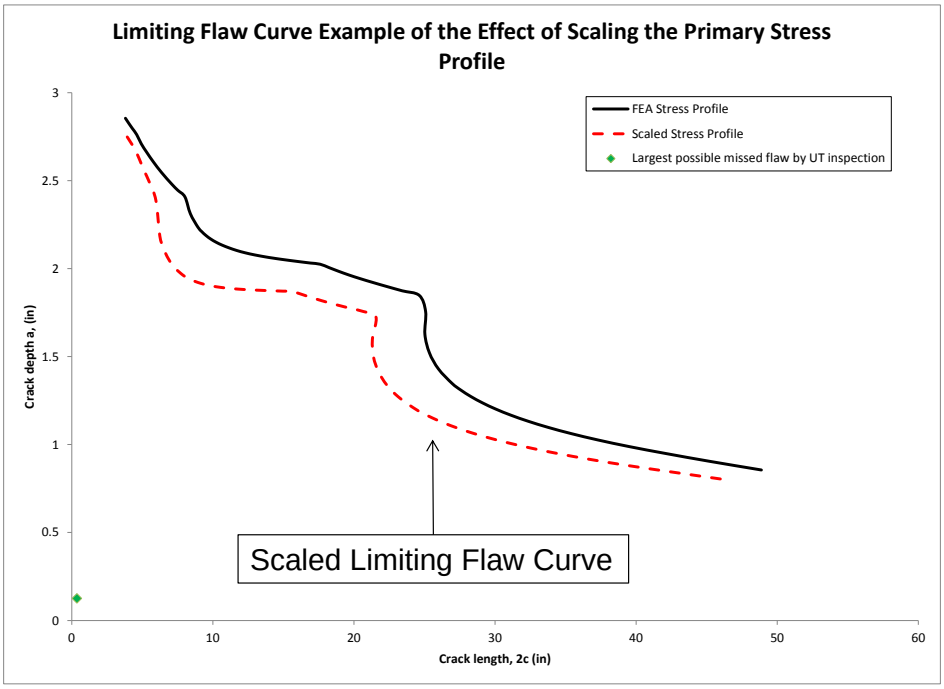

Figure 10: Scaled limiting flaw curve example.

Fatigue Driven Crack Growth

Once critical flaw sizes are determined, the next task in the damage tolerance approach is to grow a flaw to failure. The outcome of this analysis will govern how the inspection intervals are determined.

Extensive empirical data has demonstrated that the rate of fatigue crack growth in metals can be characterized by the following expression:

$$\frac{da}{dN} = \begin{cases} C\Delta K^m & \Delta K > \Delta K_{th} \\ 0 & \Delta K \le \Delta K_{th} \end{cases} \quad (1)$$

where a is a crack dimension (length or depth), da/dN is the crack growth per load cycle, ΔK is the cyclic stress intensity factor, ΔK_{th} is the threshold value of ΔK, and C & m are material constants. The *stress intensity factor*, K, is a fracture mechanics parameter that characterizes the stresses near the tip of a crack. Figure 11 illustrates the typical crack growth behavior in steels for which Equation (1) was derived.

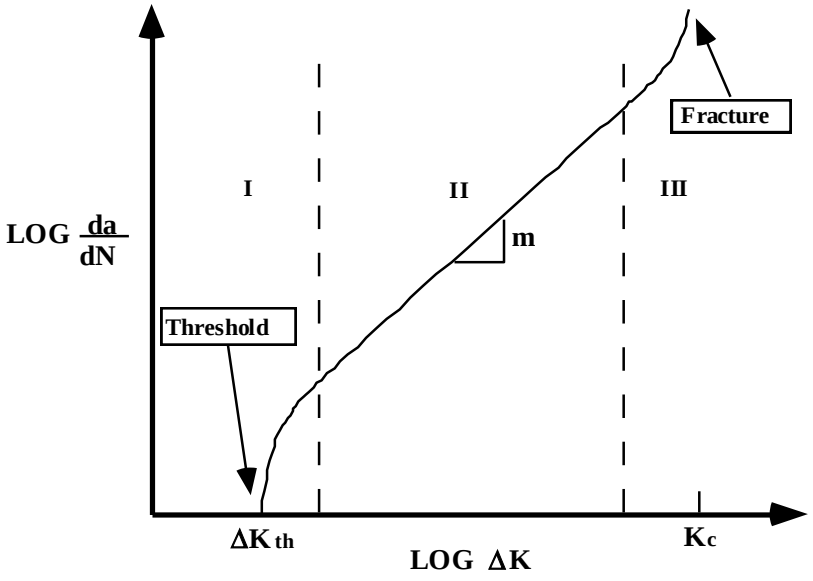

Figure 11: Typical crack growth behavior in steels

The cyclic stress intensity factor is defined as the difference between the maximum and minimum value of *K* in a given loading cycle. It is related to stress and crack size as follows:

$$\Delta K = Y \Delta \sigma \sqrt{\pi a} \tag{2}$$

where *Y* is a geometry factor that depends on the crack dimensions as well as the size and shape of the component; $\Delta\sigma$ is the cyclic stress.

Histograms of the operational modes at RPS were developed based on pressure-time measurements provided by TVA. Because the loading is variable in amplitude, rainflow counting per the ASTM standard [8] was used to correctly define the cycles to be used in the histogram. Furthermore, due to variable amplitude loading, a weighted average cyclic stress needs to be computed from the histogram by the following relationship:

$$\Delta \bar{\sigma} = \left(\frac{\sum_{i=1}^{n} \Delta \sigma_i^{\,m} N_i}{N_{tot}} \right)^{1/m} \tag{3}$$

where N_i is the number of cycles in a given histogram bin, N_{tot} is the total number of cycles in the histogram, and *m* is the exponent found in Equation (1). Note that Equation (1) includes a threshold, ΔK_{th}, below which the crack growth rate is zero. Consequently, some of the load cycles will not contribute to fatigue damage because ΔK is below the threshold. The threshold cyclic stress is given by

$$\Delta \sigma_{th} = \frac{\Delta K_{th}}{Y \sqrt{\pi a}} \tag{4}$$

Cyclic stresses below $\Delta\sigma_{th}$ are not included in the summation in the numerator of Equation (3), but *all* cycles are counted in N_{tot}. Note that $\Delta\sigma_{th}$ decreases as the crack grows larger. Thus $\Delta\bar{\sigma}$ must be recomputed at each time step.

The weighted average stress can be used to compute an average growth rate for the histogram:

$$\frac{d\bar{a}}{dN} = C\left(Y\Delta\bar{\sigma}\sqrt{\pi a}\right)^m \tag{5}$$

Life assessment for variable amplitude loading can be performed by integrating Equation (5). The number of loading cycles required to grow the crack from an initial flaw size, a_o, to a final size, a_f, is given by:

$$N = \frac{1}{C\pi^{m/2}} \int_{a_o}^{a_f} \frac{da}{Y\Delta\bar{\sigma}^m a^{m/2}} \tag{6}$$

Figure 12 illustrates an example of a grow-to-failure plot for a crack growth analysis.

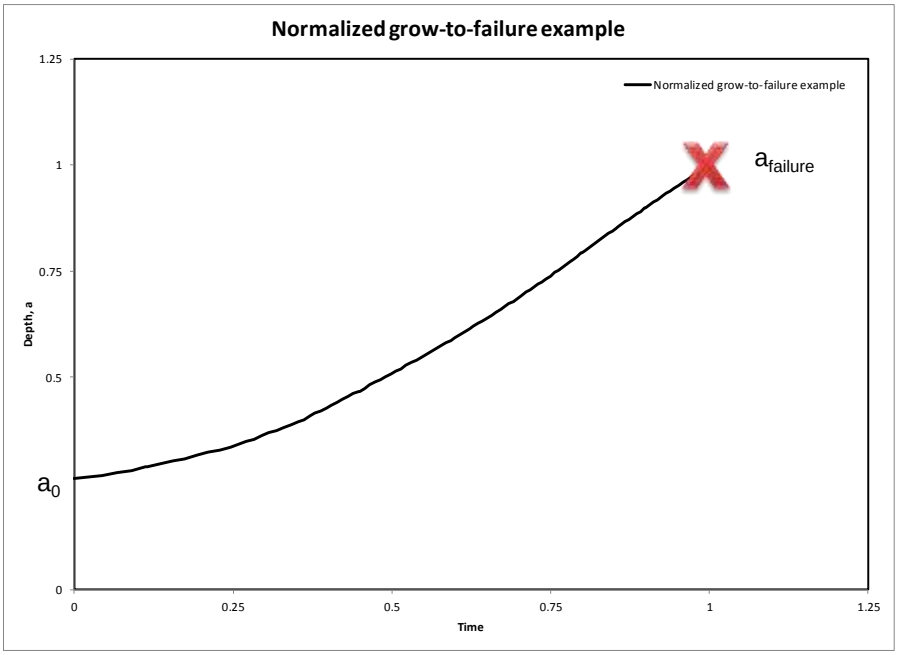

Figure 12: Example of a crack “grow-to-failure” plot.

Advanced programming or the use of custom software is needed for both the limiting flaw and crack growth analyses. Signal™ Fitness-For-Service [9] software, a verified and commercially available FFS software package developed by Quest Integrity, was used in this project.

Inspection Plan

After the “life” of the component has been estimated from the crack growth assessment, the final step in the *damage tolerance* approach is to determine inspection intervals.

The fitness-for-service method is closely tied to nondestructive evaluation (NDE). NDE provides input for both the limiting flaw and crack growth analyses. This in turn helps define inspection intervals. Further, any flaws that might be detected during an inspection can be evaluated directly using the limiting flaw charts for acceptability (see Crack Stability and Limiting Flaw Curves) and inspection intervals can be re-evaluated to ensure that the measured flaw size will not grow to failure between inspections.

The main purpose of any damage tolerance assessment is to ensure that flaws will not grow to failure between inspections. The precise methods for achieving this goal depend on practical circumstances. For example, TVA is currently budgeting for an eight-to-ten year window between major disassembly/overhauls at RPS. In this case, the FFS assessments were evaluated against the desired inspection interval targets for acceptability.

The following describes a basic overview for the determination of the inspection intervals. Critical locations of the component are identified using stress and FFS analyses; this provides targeted or focused inspection points along the component. The initial flaw size is set at an assumed value a_o, which corresponds to the largest flaw *that might be missed* by NDE. This flaw size should not be confused with the NDE detectability limit, which is the smallest flaw *that can be detected* by the NDE technique (on a good day). In most cases, a_o is significantly larger than the detectability limit, due to the variability in inspection method and the skill of the inspector. Next, the flaw is grown-to-failure (Figure 12). Inspection intervals are developed based on the acceptability and to fit within the desired outage schedule as described above. For example, Figure 13 illustrates an inspection interval based on “half-life”. If the outage requirements are within that window, then there is an approximate factor of safety of two on time-to-failure.

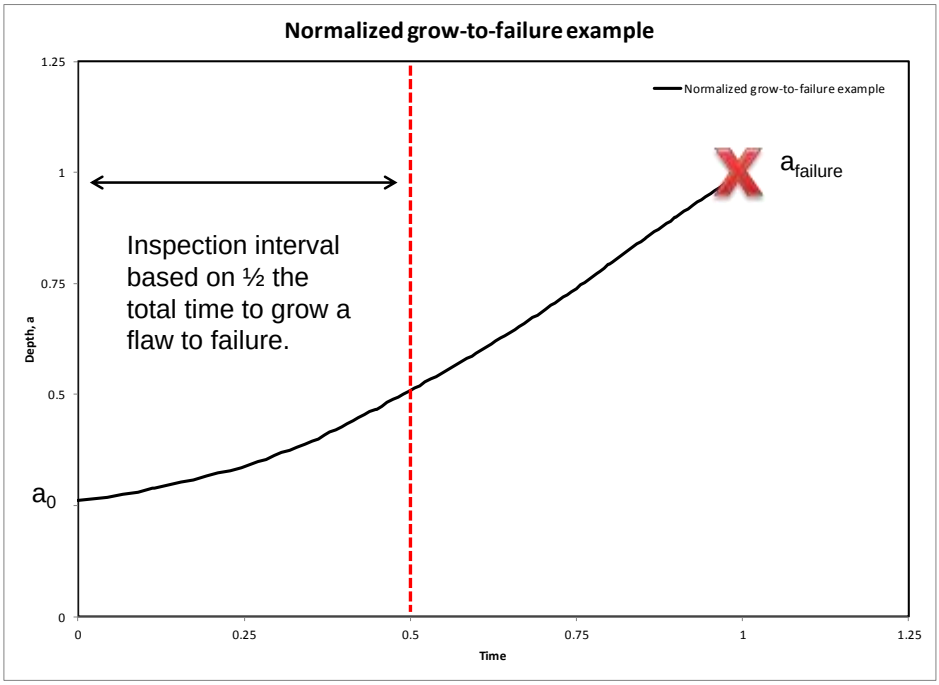

Figure 13: Example of inspection interval.

Inspection methods (e.g. wet fluorescence A/C magnetic particle, longitudinal or phased array ultrasonics (UT), etc.) based on industry best practice were recommended depending on location, access to inspection point and type of material to be inspected.

Results

The following Sections detail the results from the global and local CFD submodeling, the FEA stress analysis, the FFS assessment, and the resulting inspection plan for the spiral case.

Computational Fluid Dynamics

Although a system-wide study has been performed for the RPS project, this section of the paper focuses on a sample of key cases. A system-wide overview of the CFD results is provided for both power generation and pumping global models, while the remaining sections are generally focused on the results that were obtained along the spiral case assembly.

Global CFD Results

Two global models were developed to obtain the overall pressure and velocity distributions along the main flow path of a Francis unit while operating under power generation and pumping modes. These models were validated against pressure measurements taken at key locations along the spiral case and draft tube, as well as power usage or output (depending on the unit's operating mode).

Figure 14 shows the comparison between the predicted static pressure distributions for the unit while operating under power generation and pumping modes. Large pressure values were generally encountered along the spiral case of the unit; this was expected as a pressure drop across the runner implied the energy was being extracted from the flow, while the opposite (i.e., pressure rise across the runner) indicted that energy was being applied to the flow. The spiral case was expected to generally have the highest pressure values since the flow direction was switched depending on the operating mode of the unit. Furthermore, Figure 14 also shows higher pressure values encountered when operating under the power generation mode. For this particular reason the subsequent CFD submodeling and FEA modeling looked at the unit when operating under power generation as the predicted pressure loading was more conservative.

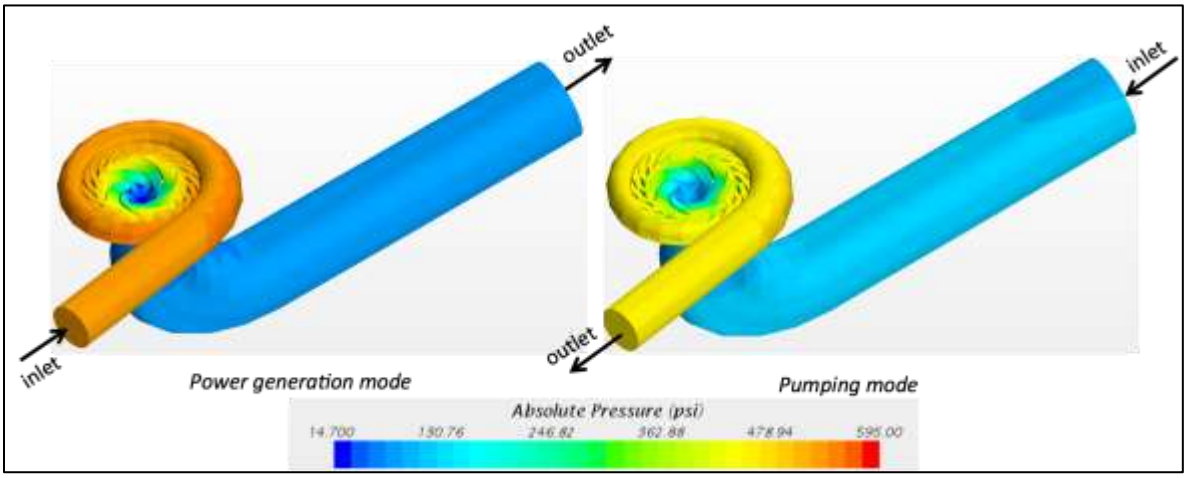

Figure 14: Power generation vs. pumping mode – static pressures (psi).

A comparison of the tangential velocity distribution within the unit between for the two analyzed operating modes is presented in Figure 15 in the form of streamlines curves. This figure shows that the global model predicted highly turbulent flow downstream of the runner for both cases. A large vortex structure known as vortex rope was predicted downstream of the runner when operating under the power generation mode. The

vortex rope is commonly present in Francis units and is normally associated with pressure fluctuations located downstream of the runner; the pressure fluctuations can happen due to due to the unsteadiness of the vortices as well as the potential for cavitation along its core. Vortex rope structures can causes significant mechanical damage depending on the magnitude of these pressure fluctuations. Figure 15 also shows that the highest velocities were encountered along the rotating surfaces of the runner.

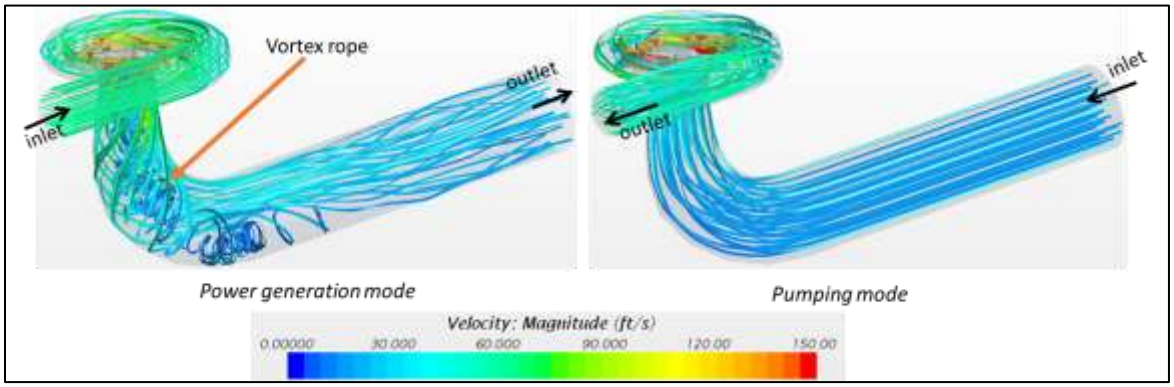

Figure 15: Power generation vs. pumping mode – streamlines (ft/s).

Spiral Case CFD Results

Figures 16 and 17 show close-up views of the pressure distribution along the spiral case, stay vanes, and stay ring of the unit while operating during power generation mode. Both figures show that high pressures values were encountered along the outer walls of the spiral case where the flow was generally slowed down; lower pressure values were encountered in between stay vanes where the flow accelerated on its way towards the runner of the unit. High pressure values were also predicted along the crotch section of the spiral case as shown in Figure 17.

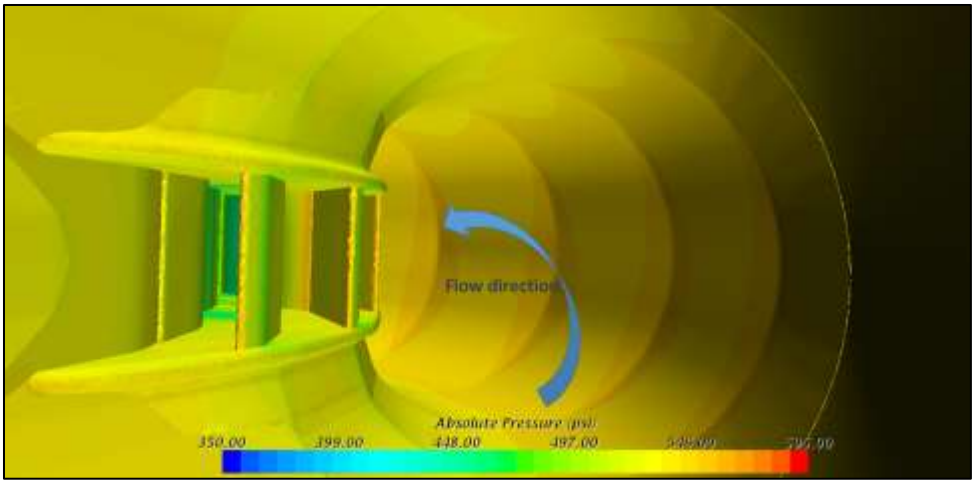

Figure 16: Static pressure inside spiral case, looking downstream (generation mode, psi).

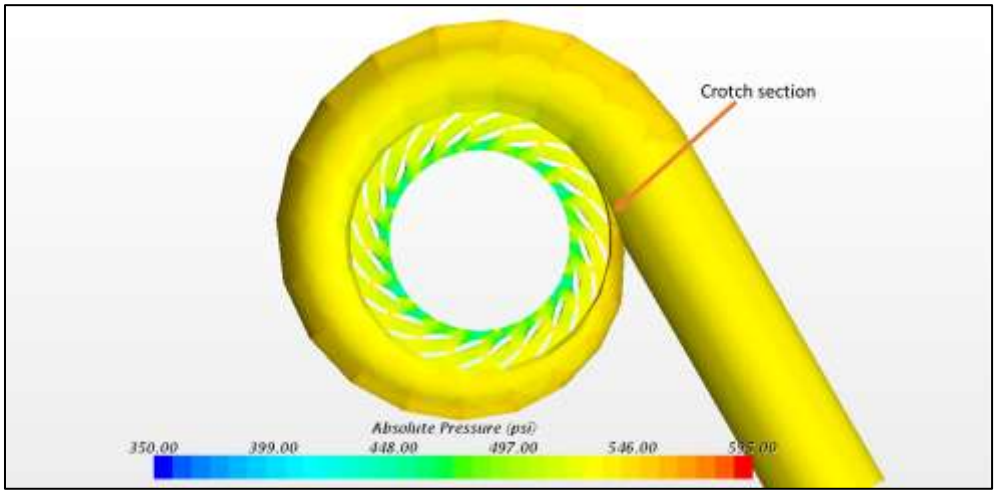

Figure 17: Static pressure on spiral case and upper stay ring (psi).

Stress Analysis of the Spiral Case

The purpose of the spiral case is to deliver water to the distributor or runner. The cross-sectional area of the spiral case decreases in the direction of flow (Figure 18). Typically in design, the concrete surrounding the spiral case is not considered to provide additional support when determining necessary shell thickness [10].

Stress and fitness-for-service analyses of the spiral case were conducted with and without the presence of the surrounding concrete. This evaluated the effects of the surrounding concrete to ensure that stresses used for subsequent FFS assessments

were not only appropriate, but represented the most accurate physical response of the system when subjected to the operational loads.

It should also be noted that the spiral case manway was modeled using a “submodel” approach in a separate analysis. This allowed for computational savings and additional mesh refinement as necessary to capture through thickness stresses in the manway casting for subsequent fitness-for-service assessments.

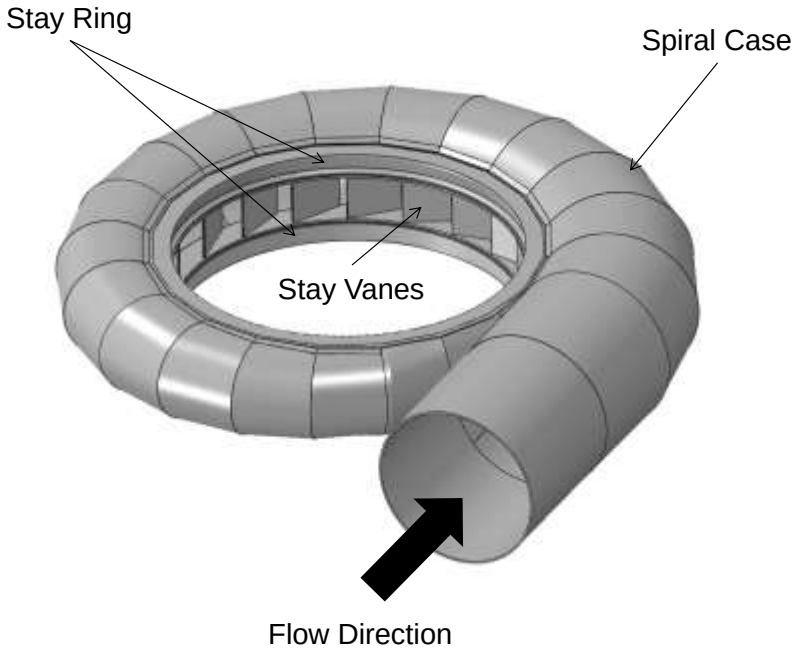

Figure 18: FEM of spiral case, stay rings and stay vanes.

The spiral case is constructed with a series of circumferential plates of varying thicknesses and curvatures. Figure 19 illustrates the various shell sections that comprise the spiral case found at RPS.

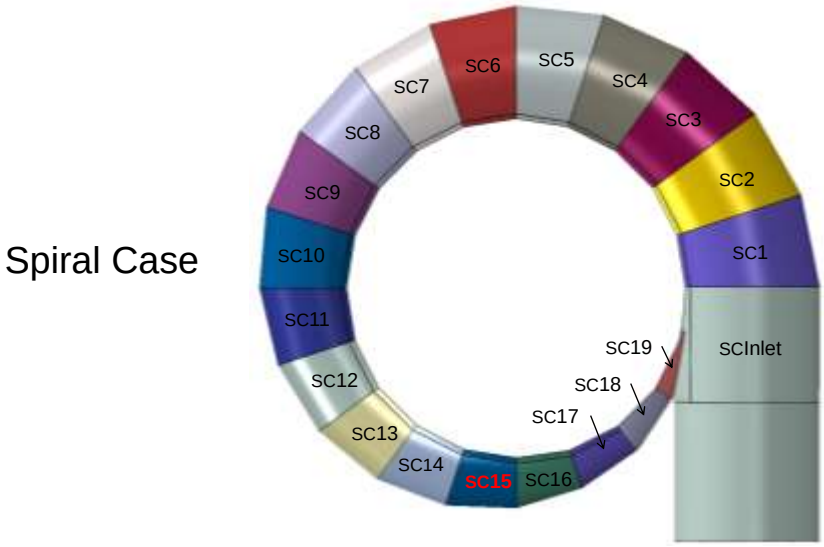

Figure 19: Shell sections of spiral case.

Many of the shell sections are connected to the stay ring by transition joints as shown in Figure 20. It should be noted that the finite element “mesh lines” and the surrounding concrete were removed in most of the figures for viewing clarity.

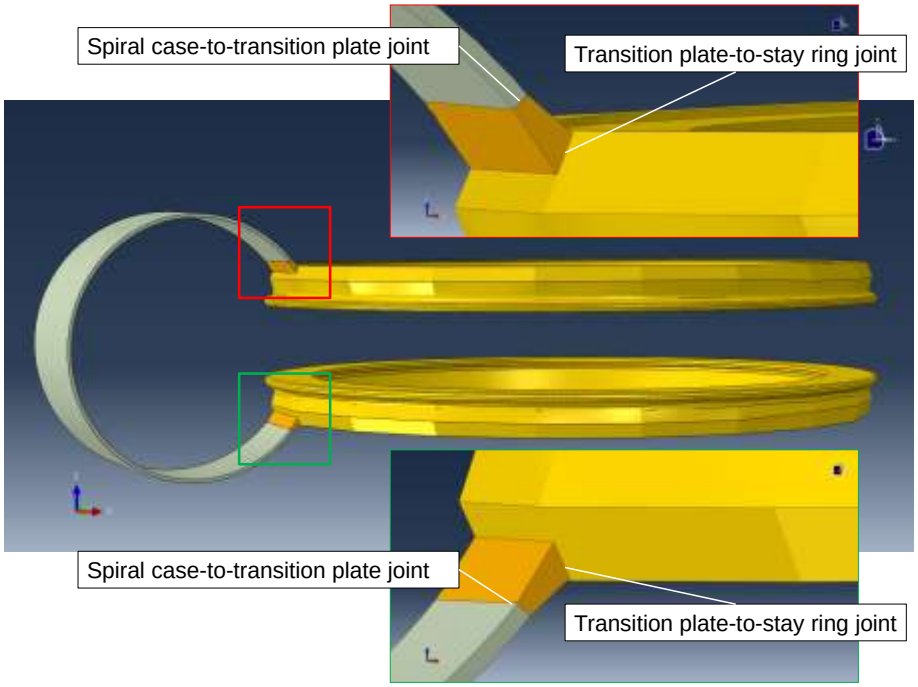

Figure 20: Spiral case transition joints.

Pressures from the CFD analyses were mapped to the FEM of the spiral case (Figure 21) and the stresses were computed using the Abaqus [7] FEA solver. The results confirmed that peak stresses in the spiral case were below the von Mises yield criteria (Figure 22). The shell and transition joint material was constructed from ASTM A517 Grade F which has yield strength of 100 ksi. This verified linear elastic response within the structure and validated the modeling approach.

Had stress values exceeded the von Mises yield criteria an elastic-plastic stress analysis would have been proposed. Those results would then be evaluated to ensure that the structure is protected against plastic collapse, or gross cross-sectional instability, and any local plastic strains which might have accumulated due to cyclic loading, otherwise known as ratcheting.

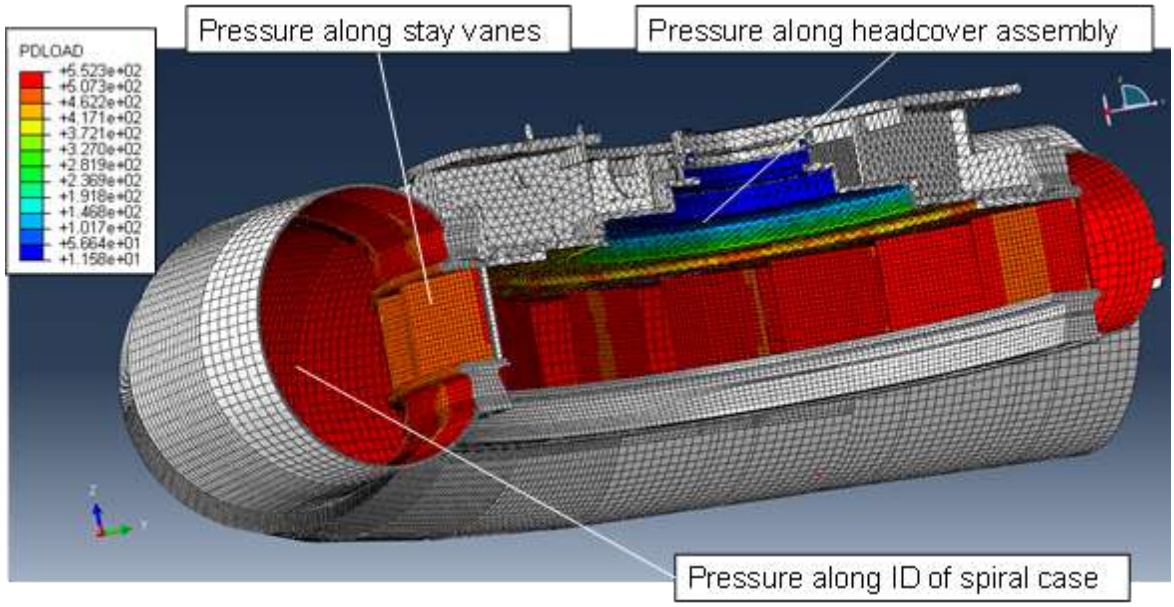

Figure 21: Pressure results from CFD mapped to spiral case FEM (psi).

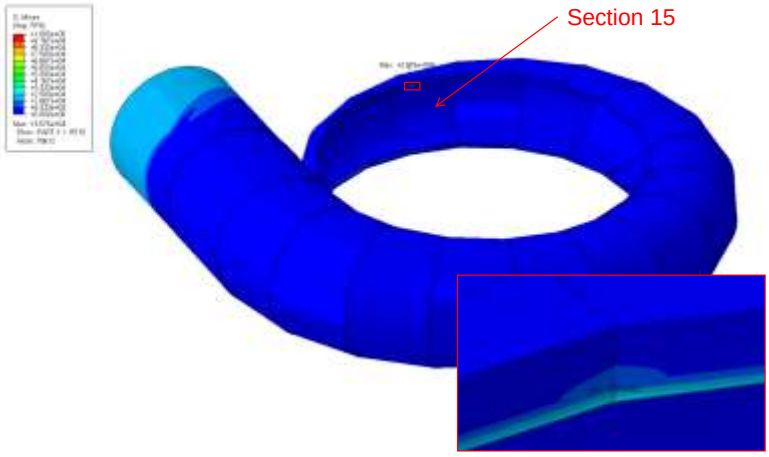

Figure 22: Von Mises stress contours in spiral case (psi).

The peak stress location was identified along the upper transition joints in Section 15 of the spiral case where the spiral case is joined to stay ring (Figure 22). The maximum absolute principal stress in Section 15 was evaluated to determine the critical stress plane. Should a crack-like flaw be oriented with the crack face parallel to the critical stress plane, the local stress normal to that plane would provide the maximum crack driving force. In this particular example the maximum absolute principal stress occurred mostly in the hoop or circumferential direction (Figure 23).

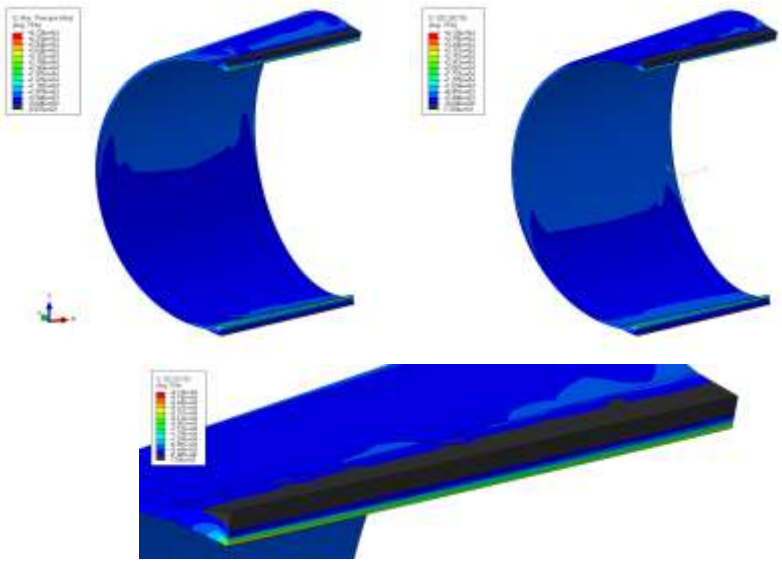

Figure 23: Stress contours local to shell segment (psi).

Fitness-for-Service of the Spiral Case

Based on the stress analysis, the most likely scenario for the formation and propagation of a crack like flaw would occur along the weld that joins Section 15 of the spiral case to the stay ring (Figure 24).

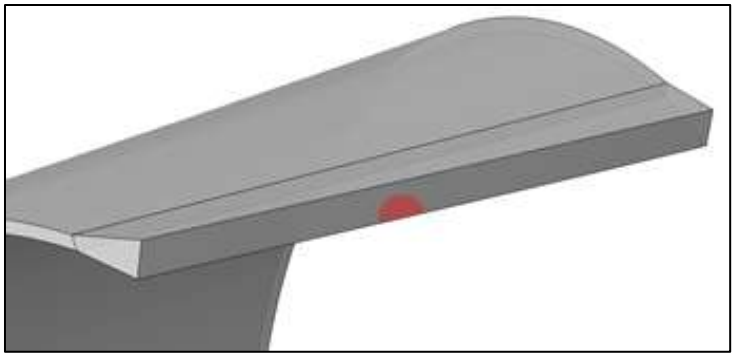

Figure 24: Probable location of crack like flaw.

Crack Stability and Limiting Flaw Curves

Upper bound primary through thickness stress profiles that occurred at the maximum stress location in Section 15 of the spiral case, conservative weld residual profiles, and lower bound yield, ultimate and fracture toughness values were used for the limiting flaw analyses to maintain appropriate conservatism (Table 2).

Table 2: Material properties used for the FFS assessments.

Component	Material	Yield Strength (ksi)	Tensile Strength (ksi)	Fracture Toughness ($ksi\sqrt{in}$)
Stay Ring	ASTM A516 Gr.70 plate[1]	38	70	105
Spiral Case	ASTM A517 Type F plate	110	115	105[2]

[1] The plates were manufactured in accordance to the ASTM A516 standard which requires plate thicknesses of greater than or equal to 1.5inches to be normalized. Normalization of the material increases the overall fracture toughness.

[2] A fracture toughness value for the spiral case transition joint was assumed to be equivalent to the lower bound weld and adjoining stay ring material to maintain appropriate conservatism.

Material testing is the preferred way to determine *actual* material properties of a component. However, extracting a consumable material test specimen from an in-service component may not be practical. Alternative methods of determining material properties exist, for example: comprehensive literature search or lower bound assumptions following the guidelines found in Annex F of the ASME FFS-1 [2] standard. Unless confidence in the values found in literature is high, it is best to at conduct the analyses with lower bound assumptions found in the ASME FFS-1 [2] standard.

A comprehensive literature search for toughness values for ASTM A517 Type F plate, also referred to as T1 from USS [11] trade name, revealed a toughness value of 140 $ksi\sqrt{in}$ at 50°F. Although ASTM A517 Type F displayed upper bound material properties, it has been found to be prone to hydrogen cracking in the heat affected zone (HAZ) of welds. Hydrogen could be introduced through contaminated weld filler material. Until actual material tests can be conducted, a lower bound fracture toughness value equivalent to the adjoining stay ring's toughness was used in the FFS assessments.

Figure 25 represents the limiting flaw curves for the welded joint where Section 15 of the spiral case is joined to the upper portion of the stay ring calculated using Signal™ Fitness-for-Service [9] software. There are two curves represented in the plot: the black solid curve represents limiting aspect ratios for surface breaking semi-elliptical crack-like flaws; the blue dashed line represents the largest acceptable through-wall crack-like flaw. Further, the reference red point below the curve represents the largest possible flaw that might be missed in an ultrasonic inspection.

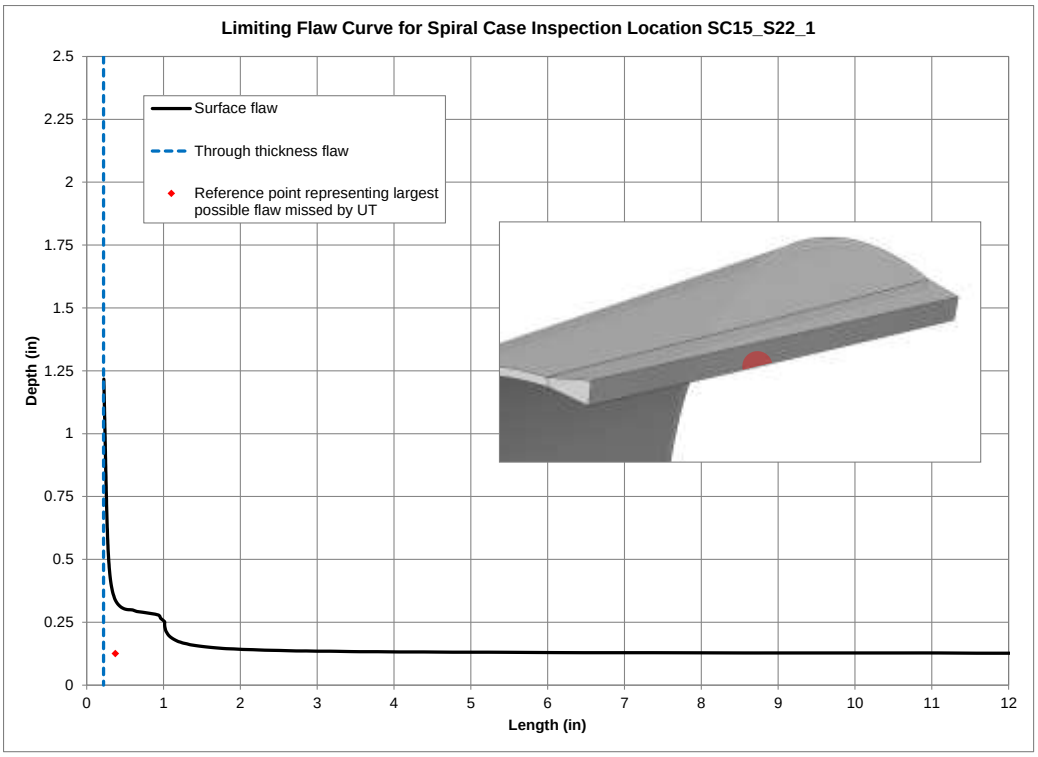

Figure 25: Limiting flaw curve for spiral case-to-stay ring welded joint

Crack dimensions that fall below the curves are considered sub-critical, whereas those that fall outside of the curves are critical. Thus, these curves represent combinations of crack lengths and depths that could pose a significant risk of sudden failure. These curves were used to determine future inspection requirements and to evaluate the stability of any measured linear indications.

Limiting flaw curves were created for the remaining sections of the spiral case following the procedures outlined above. This provided limiting flaw curve plots for inspection reference for the entire spiral case.

Fatigue Driven Crack Growth

One of the final steps in the damage tolerance approach of determining inspection intervals is to estimate the remaining life of the component by growing a flaw to failure. This procedure follows the procedure outlined in the Fatigue Driven Crack Growth Section. A “grow-to-failure” analysis consists of growing an initial flaw size using the assumed material properties and cyclic histogram until the flaw becomes unstable. The point of instability, or failure, is where the final crack dimensions are on or outside

limiting flaw curve. It was determined that Section 15 of the spiral case would represent the limiting remaining life based on the stress and crack stability analyses conducted.

In addition to the assumptions used in the previous Section (Crack Stability and Limiting Flaw Curves) and the material properties found in Table 2, a ΔK_{th} of 2 $ksi\sqrt{in}$ and material constants of 3.6E-10 and 3 for *C* and *m* respectively, were assumed for crack growth parameters. Again, these parameters were lower bound estimates from the ASME FFS-1 [2] standard. Histograms of the operational modes at RPS that were developed (see Fatigue Driven Crack Growth) were used to "drive" the crack growth.

Using Signal™ Fitness-for-Service [9] software and the material properties and assumptions described above as inputs, a grow-to-failure analysis was conducted. Figure 26 represents the largest possible surface flaw that might be missed during an inspection using UT grown to failure. This provides an estimated remaining life of the spiral case based on the assumptions and material properties considered. Because Section 15 was considered as the limiting case, the estimated remaining life of the spiral case is forty-seven years (Figure 26).

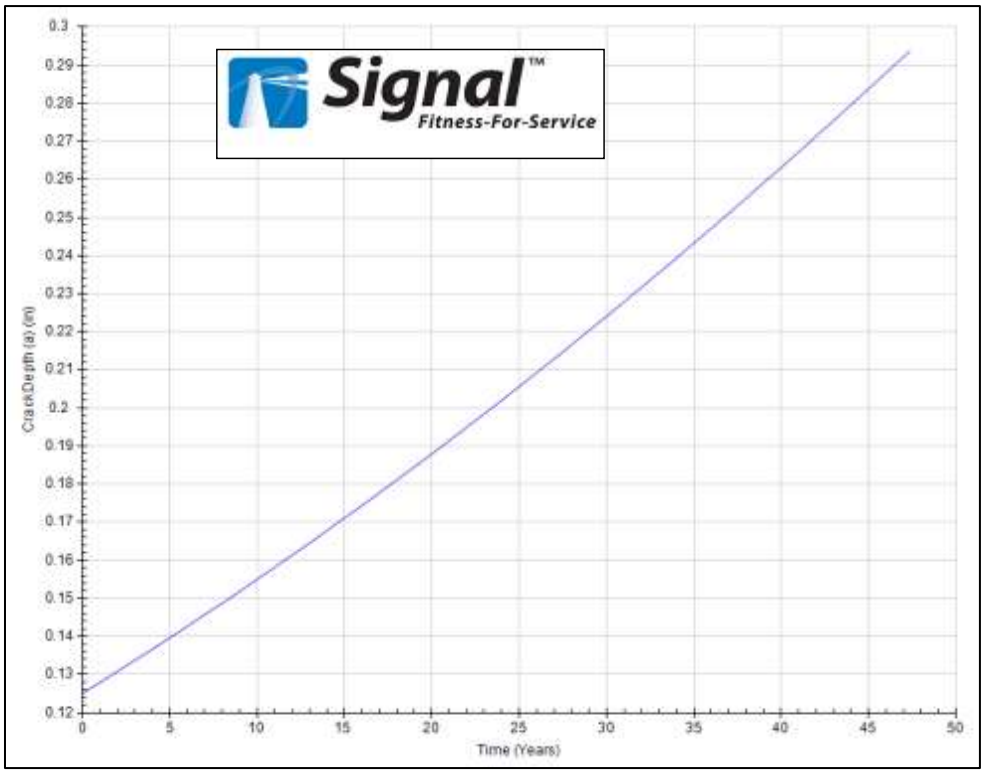

Figure 26: Crack growth-to-failure plot

Until now, fracture toughness has been described and as a single deterministic value. However, there is typically a high degree of scatter in actual material toughness data, and the actual toughness values can be higher than lower bound toughness predictions. Due to this scatter, it might be more appropriate to treat the fracture toughness as a statistical distribution rather than a single value.

For example, a lower bound material toughness value relates to a five percent probability that the fracture toughness is at or below the predicted value. If this value proved too conservative, a probabilistic approach using the master toughness curve found in the ASME FFS-1 standard [2] was used to determine an appropriate fracture toughness value.

Inspection Plan for the Spiral Case

The objective for this project was to provide TVA with details, supported by recognized engineering methods and standards, on where, when, and by what means to inspect water passage components. The inspection intervals were based on the remaining life of forty-seven years for the limiting case determined in the previous section, and the acceptability of the desired eight-to-ten year window between major disassembly/overhauls at RPS requested by TVA.

Figure 26 and Figure 27 represent stable crack growth for approximately forty-seven years, at which time the crack becomes unstable and could pose a significant risk of sudden failure. Ten years of stable crack growth (Figure 27), the desired interval for major disassembly/overhauls at RPS, is acceptable by a factor of **four** on time.

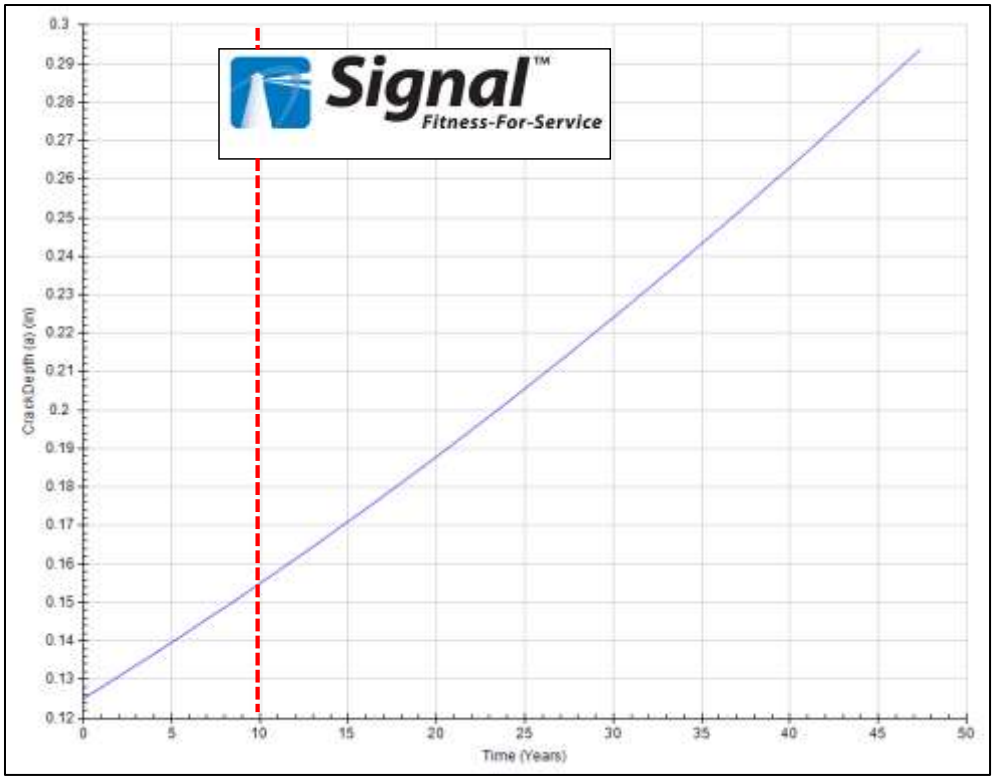

Figure 27: Dashed line represents TVA's desired inspection interval at RPS.

Stated another way, the desired interval for inspection of eight-to-ten years for major disassembly and overhauls at RPS is acceptable with a factor-of-safety on time of four.

Figure 28 represents the locations on the Section 15 of the spiral case for targeted inspection. Because the entire spiral case was evaluated, designations for inspection locations were needed. This provided more inspection detail for TVA of where to inspect and which limiting flaw curve to use for evaluation of any flaw found. For example, S22_1 in Figure 28 refers to longitudinal weld joint connecting the spiral case to the stay ring and represents the limiting case as discussed throughout this paper. Additional locations are also marked and have associated limiting flaw curves for inspection reference.

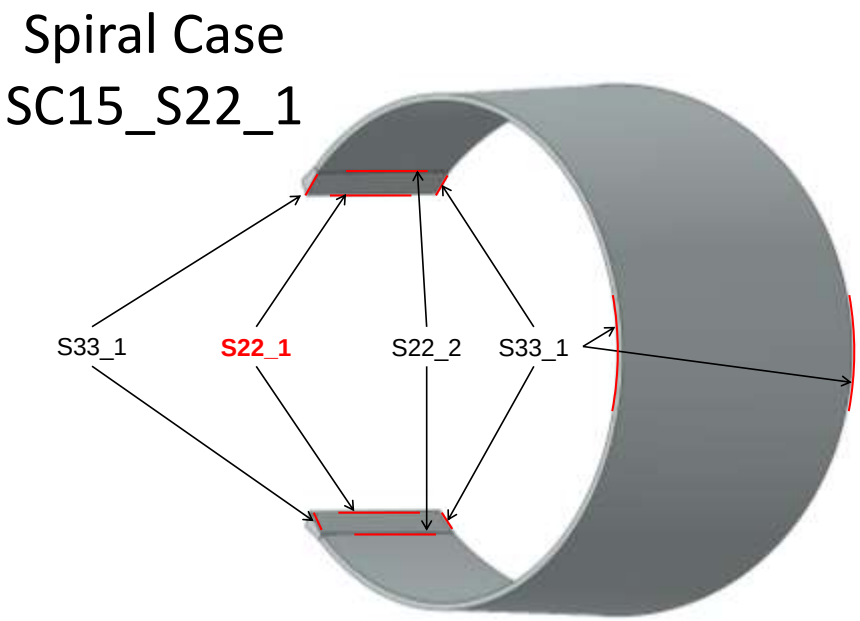

Figure 28: Inspection location in Section 15 of the spiral case.

Information in the form of component identification, referenced mechanical drawings, inspection frequency, recommended inspection methods, and additional recommendations were provide to TVA's engineering group. Figure 29 represents an excerpt from the spiral case inspection plan provided to TVA. TVA's project engineers will upload this information, along with inspection plans for the other water passage components evaluated, into TVA's Asset Management software which is shared with TVA's internal Inspection Service Organization (ISO). This provides TVA with the ability to maximize planning and budgeting for inspections of critical water passages components.

General Information	
Component:	RPS spiral case
Inspection location:	Section 15 at the spiral case-to-stay ring weld joint
Materials:	Spiral Case: ASTM A517 Type F
	Stay Ring: ASTM A516 Gr.70 (normalized)
Drawings referenced:	1006-AEZ-1 missing vane.pdf 1006-AHQ-1-SHT -REV 5.pdf 1006-AHS-1 missing vane.pdf 5112-NE-1-SHT -REV 5.pdf

Component:	**Spiral case: Section 15**	**Notes: N/A**
Damage mechanism:	**Crack-like flaws**	
Inspection procedure		**Inspection frequency**
1. Clean and prepare longitudinal weld location joining the spiral case to the stay ring.		1. Baseline inspections should be conducted within two inspection intervals (based on TVA's desired 8-10 year outage schedule).
2. Layout and mark a grid on the water side surface at the longitudinal weld location joining the spiral case to the stay ring. Permanent locator marks to allow the grid to be re-established in the future are necessary. Once marked permanently, the actual joint configuration can be interrogated with ultrasound.		
3. Interrogate the weld and recording findings relative to the established inspection grid. Longitudinal wave UT can be used for inspection. However, phased array UT will provide better flaw characterization capabilities.		
4. Map any measured flaw dimensions to the limiting flaw chart for evaluation.		

Comments

1. **Contact Quest Integrity should any flaws be discovered and before any repairs are carried out.**
2. Any measured linear or volumetric indications will need to be evaluated to determine crack stability and re-evaluate the remaining life and inspection interval.
3. Material samples may be requested.

Figure 29: Excerpt from inspection plan

Conclusion

Critical locations of the component were identified by analyzing each of the fourteen water passage components modeled through stress and FFS analyses. This approach was supported by quantitative means recognized in the ASME FFS-1 [2] engineering standard. This provided TVA with focused inspection plans for each of the components evaluated and thereby, reduced costly and time consuming general inspections which typically fail to sufficiently address the entire component.

Based on the limiting case for the spiral case described herein, TVA can meet the desired eight-to-ten year interval between major disassembly and overhauls at RPS, before a required inspection. According to TVA, the cost of this comprehensive analysis was, "*Less than the value of 2 weeks of generation on one unit*".

In addition to improving outage planning and budgeting, other benefits of the fitness-for-service approach are described below:

- Focused inspections to critical areas of components instead of a general "inspect everything" approach **improves safety** and **reduces inspection costs**.
- Evaluation of the structure's physical response to applied operation loads through stress and FFS analyses provides quantitative support to **identify actual risks** and **dispel perceived risks**.
- Evaluation of structural modifications or upgrades to components by a recognized engineering standard [2] ensures component is **fit-for-continued service**.
- A **predicative** approach using FFS method **reduces costly** and **uncertain** "11th hour" **reactions** to discovered flaws.

Authors

Eric Scheibler is a Senior Consulting Engineer with Quest Integrity Group. He specializes in fracture mechanics and finite element analysis (FEA) of a variety of structural types including static, transient, and non-linear models. Eric also specializes in fitness-for-service assessments of flawed structures to determine if repair, replacement, or continued monitoring is needed for safe operation. Eric has conducted numerous engineering critical assessments on fixed and rotating equipment within the power generation, petrochemical and petroleum industries.

Bruno Fletcher is a CFD Consulting Engineer with Quest Integrity Group. He specializes in Computational Fluid Dynamics (CFD) and Heat Transfer modeling. He has previously worked as a Thermal Analyst for Lockheed Martin for the Space Shuttle program and as a CFD consultant for CD-adapco where his work was focused on performing flow modeling for the Power and Petrochemical industries. Bruno has conducted CFD modeling on multiple hydro and gas turbine units. He has a Master of Science degree in Aerospace Engineering from Embry-Riddle Aeronautical University.

References

[1] [Online]. http://www.tva.gov/sites/raccoonmt.htm

[2] The American Petroleum Institute and the American Society of Mechanical Engineers, "Fitness-For-Service," *Fitness-for-Service API 579-1/ASME FFS-1*, p. 1128, June 2007.

[3] Dassault Systèmes. SolidWorks Premium, x64 SP5.0 ed. www.simulia.com.

[4] McNeel & Asscoiates. Rhinoceros v5. http://www.rhino3d.com/.

[5] CD-adapco. Star-CCM+ 8.02.011. http://www.cd-adapco.com/products/star_ccm_plus/.

[6] M. McLinden, D. Friend E. Lemmon, "Thermophysical Properties of Fluid Systems," in *NIST Chemistry WebBook, NIST Standard Reference Database*.: National Institute of Standards and Technology, 2011, ch. Number 69.

[7] Dassault Systèmes. Abaqus 6.13. www.simulia.com.

[8] ASTM International, "Standard Practices for Cycle Counting in Fatigue Analysis," *E1049-85 (Reapproved 2011)*, p. 10, October 2011.

[9] Quest Integrity Group, LLC. Signal Fitness-for-Service Software, V.4.0. www.QuestIntegrity.com.

[10] Hydro Power Technical Committee American Society of Mechanical Engineers, *The Guide to Hydropower Mechanical Design*. Kansas City, USA: HCI Publications, 1996.

[11] United States Steel Corporation, T1 Constructional Alloy Steels, 1985.